Metabolic Brain Disease (2025) 40:161
https://doi.org/10.1007/s11011-025-01581-2

RESEARCH

Hydroxysafflower yellow A alleviates the inflammatory response in astrocytes following cerebral ischemia by inhibiting the LCN2/STAT3 feedback loop

Lijuan Song[1,2,3] · Yige Wu[2] · Lijun Yin[2] · Yanzhe Duan[2] · Jianlin Hua[2] · Mengwei Rong[2] · Kexin Liu[2] · Junjun Yin[2] · Dong Ma[3] · Ce Zhang[1] · Baoguo Xiao[4] · Cungen Ma[2,3]

Received: 16 December 2024 / Accepted: 17 March 2025 / Published online: 26 March 2025

Abstract

Lipocalin-2 (LCN2), an acute phase protein mainly expressed in astrocytes (Ast), is closely related to the production of inflammatory cytokines following ischemic stroke. During the pathophysiological process of ischemic stroke, the Janus kinase 2/signal transducer and activator of transcription 3 (JAK2/STAT3) signaling pathway is activated. Despite evidence suggesting some link between the two, the relationship between the JAK2/STAT3 signaling pathway and the LCN2 expression in Ast following brain ischemia is incompletely understood. Hydroxysafflower yellow A (HSYA), an active ingredient found in Carthamus tinctorius L flowers, has been demonstrated to effectively mitigate cerebral ischemia via its anti-inflammatory effect. However, whether HSYA mitigates the neuroinflammatory damage after ischemic stroke by disrupting the interaction between the JAK2/STAT3 signaling pathway and LCN2 in Ast is unknown. Focusing on these two scientific questions, we established an in vivo middle cerebral artery occlusion/reperfusion (MCAO/R) rat model and in vitro primary astrocyte oxygen glucose deprivation/reperfusion (OGD/R) model. In vivo results showed that HSYA treatment alleviated nerve damage and inhibited the expression of LCN2 and inflammatory factors in Ast. In vitro results showed after OGD/R the expression of LCN2 and inflammatory cytokines increased and the JAK2/STAT3 was activated in Ast. Meanwhile, after OGD/R the JAK2/STAT3 activation in Ast increased LCN2 expression, and the inhibition of LCN2 expression by HSYA decreased the JAK2/STAT3 activation in Ast. These findings suggest that there is an interaction between the LCN2 and JAK2/STAT3 in Ast after ischemic stroke, which can enhance the inflammatory factors and exacerbate neuroinflammatory injury. Therefore, we conclude that HSYA may inhibit the LCN2/STAT3 loop in Ast, thereby mitigating neuroinflammation after cerebral ischemia.

Keywords Hydroxysafflower yellow A (HSYA) · Inflammatory response · Astrocyte · Cerebral ischemia · LCN2/STAT3 loop

✉ Ce Zhang
cezh@sxmu.edu.cn

✉ Baoguo Xiao
bgxiao@shmu.edu.cn

✉ Cungen Ma
macungen@sxtcm.edu.cn

[1] Department of Physiology, Shanxi Medical University, Taiyuan, China

[2] The Key Research Laboratory of Benefiting Qi for Acting Blood Circulation Method to Treat Multiple Sclerosis of State Administration of Traditional Chinese Medicine/ Research Center of Neurobiology, Shanxi University of Chinese Medicine, Jinzhong, China

[3] Department of Neurosurgery, Sinopharm Tongmei General Hospital, Datong, China

[4] Institute of Neurology, Huashan Hospital, Institutes of Brain Science and State Key Laboratory of Medical Neurobiology, Fudan University, Shanghai, China

Introduction

Acute ischemic stroke is a devastating neurological disorder with high morbidity and severe mortality (Ajoolabady et al. 2021). Accounting for more than 80% of all strokes, acute ischemic strokes are largely caused by the occlusion of arterial vessels (Paul and Candelario, 2021). Neuroinflammation plays a crucial role in the pathophysiological progression and clinical outcome of ischemic stroke (Lucas et al., 2006; Xu et al. 2020). In particular, astrocytes (Ast)-mediated inflammation following ischemic and hypoxic events has drawn much research interest (Suk 2016; Luo et al. 2022). In this process, Lipocalin-2 (LCN2), a member of the secreted lipocalin family and an acute phase protein closely related to inflammatory cytokines, seems to play an important role (Ranjbar et al. 2019). For example, LCN2 is found to be involved in cerebral ischemia, activating Ast to induce the infiltration of neutrophils and macrophages into the brain and regulating inflammatory mediators and chemokines, such as nitric oxide synthase (iNOS), interleukin (IL)−6, IL-8, and tumor necrosis factor (TNF)-α (Kido et al. 2020; Zhong et al. 2021; Liu et al. 2022a). However, the role of LCN2 in Ast-mediated inflammation following ischemia and hypoxia is still unclear.

The Janus kinase 2/signal transducer and activator of transcription 3 (JAK2/STAT3) pathway is a cytoplasmic signaling pathway closely associated with cancer, inflammation, and abnormal immunoreaction. Previous studies have shown that the JAK2/STAT3 pathway remains dormant under physiological conditions and is activated during the pathological process of cerebral ischemia. It also responds to various pathogenic factors, such as inflammation, oxidative stress, and cell apoptosis, and JAK2/STAT3 molecules are highly expressed in neurons and glial cells in proximity to the infarction (Wang et al. 2021; Zhao et al. 2023). Hypoxia caused by cerebral ischemia may activate the JAK2/STAT3 pathway, leading to an expansion of the cerebral infarction and neurological impairment (Zhang et al. 2023). Inhibition of JAK2/STAT3 phosphorylation was found to reduce microglial and Ast activation, decrease inflammatory cytokine secretion, and promote neural repair following brain injury (Zhong et al. 2022). Similarly, treatment with ginkgo biloba extract (GB) reduced LCN2 expression by reducing STAT3 and JAK2 phosphorylation, thereby inhibiting Ast activation following cerebral ischemia (Adly et al. 2021). On the contrary, development of an inflammatory microenvironment induces the secretion of LCN2 from activated microglia and Ast, thereby activating the JAK2-STAT3 and subsequently stimulating the release of inflammatory cytokines (Adly et al. 2021; Ha et al. 2022). Despite this knowledge, the relationship between the JAK2/STAT3 pathway and the expression of LCN2 in Ast following brain ischemia remains incomplete. Importantly, it is unclear whether there is feedback interaction between LCN2 and the JAK2/STAT3 following the development of ischemia and hypoxia, a question that the current report attempted to answer.

Hydroxysafflower yellow A (HSYA) is an active ingredient found in Carthamus tinctorius L flowers, a traditional Chinese medicine used in the management of ischemic stroke. Preclinical research found that HSYA has multifaceted pharmacological effects, including anti-inflammatory, antioxidant, anti-apoptotic, blood-brain barrier protective, angiogenesis-promoting, reparative, and synaptogenesis-facilitating effects (Zhang et al. 2022; Sun et al. 2018). In our previous study, it was found that HSYA exerts neuroprotection by suppressing neuroinflammatory damage through inhibition of the JAK2/STAT3 in microglia following ischemic stroke (Wei et al. 2022) and actively engaging in neuronal autophagy following OGD/R (Wei et al. 2022). Further investigation is needed to determine whether HSYA can mitigate neuroinflammatory damage after ischemic stroke by disrupting the interaction between the JAK2/STAT3 and LCN2 in astrocytes.

Materials and methods

Bibliometric analysis

Bibliometric analyses were conducted utilizing the WoS CC bibliographic database, developed by Thomson Scientific for SCI extension, to ensure a comprehensive and systematic retrieval of relevant literature. The search strategy encompassed the timeframe from 2011 to 2024, with a spotlight on the pivotal terms ‘STAT3’, ‘liposomal protein-2 (LCN2)’, and ‘astrocyte’. It employed a targeted approach using the following search parameters: (Topic=(‘Signal Transducer and Activator of Transcription 3’ OR ‘STAT3’)) AND Topic=(Astrocyte) AND (Topic=(‘Lipocalin-2’ OR ‘LCN2’)) AND Topic=(Astrocyte). This method is designed to pinpoint the confluence of these fields of research through comprehensive searches. The search was refined to include only English-language articles and review papers, ensuring linguistic consistency and interpretability of the results. Duplicate, non-peer-reviewed, and irrelevant publications were manually excluded to maintain the integrity and relevance of the dataset. The processed data were analyzed using CiteSpace and VOSviewer, two software tools known for their capabilities in visualizing and analyzing scientific knowledge networks and co-citation patterns. These tools facilitated the identification of research trends, collaboration networks, and structural evolution of the field over time.

High-performance liquid chromatography (HPLC) analysis of HSYA

HPLC analyses were performed using an Apollo C18 column (250 mm×4.6 mm, 5 μm; Grace Davison) on a LC-10AT HPLC chromatographic system with a SPD-6AV ultraviolet (UV) detector (Shimadzu; Kyoto, Japan). The mobile phase consisted of acetonitrile (A) and 0.1% trifluoroacetic acid (B) at a flow rate of 1.0 mL/min. The gradient elution program was as follows: an initial eluent of 1% solvent A, 99% solvent B; from 0 to 50 min, solvent A was linearly increased from 1 to 35%, and solvent B was linearly decreased from 99 to 65%; and from 50 to 60 min, solvent A was linearly increased from 35 to 45%, and solvent B was linearly decreased from 65 to 55%. The optical absorbance was monitored at 405 nm and the column temperature was 30 °C. The purity of HSYA was quantitatively determined by the area normalization method (Fig. 1).

Animals, MCAO/R model, and HSYA treatment

Forty-eight adult male Sprague-Dawley rats (body weight: 200–230 g) were purchased from Beijing Vital River Experimental Animal Technology Co., LTD. Animal experiments were conducted in accordance with the experimental animal ethical principles formulated by the Biomedical Ethics Review Committee of Shanxi University of Chinese Medicine (Approval No: 2020DW081).

After anesthesia with pentobarbital sodium (50 mg/kg), the common carotid artery, internal carotid artery, and one external carotid artery were surgically exposed. The internal carotid artery was clamped, and ophthalmic scissors were used to make a small cut in the common carotid artery. The fishing line was inserted and pushed into the internal carotid artery. The internal carotid artery was then unclamped, and the fishing line was pushed into the middle cerebral artery without further movement. After 2 h, the rats were anesthetized again, the original incision was re-exposed, and the fishing line was pulled out to establish reperfusion before closing the wound with sutures. After the operation, the rats were returned to the cage and given adequate food and water. Rats were sacrificed within 24 h of removal of the fishing line.

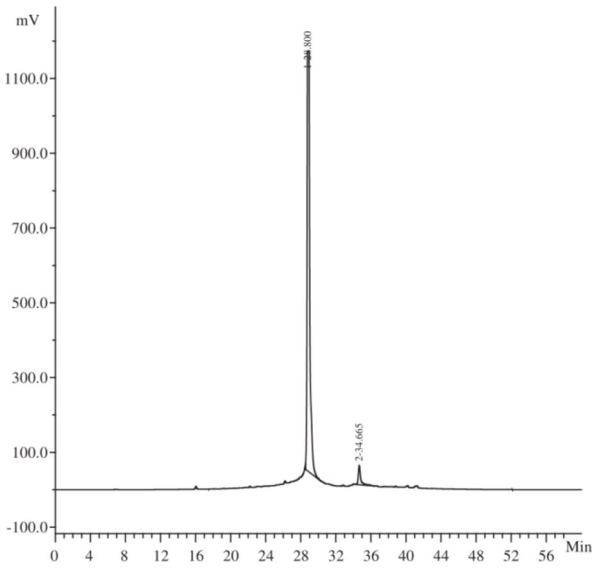

Fig. 1 HPLC analysis of HSYA. The absorbance was measured at 405 nm. The peak at 28 min is HSYA. The purity of HSYA was 95.9%

Rats in the sham group received similar surgical procedure with the exception that only blood vessel separation was performed without vessel ligation. In the treatment group (MCAO/R + HSYA), the procedure was performed as in the MCAO/R group, with an intraperitoneal injection of HSYA (12 mg/kg) given upon removal of the fishing line.

Primary Ast, OGD/R model, and HSYA treatment

The cerebral cortex of C57BL/6 neonatal mice was harvested under aseptic conditions within 24 h of birth. The meninges and blood vessels were removed from the brain tissue in high glucose Dulbecco's Modified Eagle Medium (DMEM). Cell suspensions were formed by pipetting and blowing with a straw. Centrifugation was carried out at 4 °C and 300 × g/min for 10 min, and the supernatant was discarded. This process was repeated two more times. Centrifugation was performed using a 100 μm cell strainer, and the supernatant was discarded. The cell pellet was resuspended in high glucose DMEM containing 10% fetal bovine serum and 1% penicillin-streptomycin mixture and then inoculated in cell culture flasks coated with poly-lysine. The flasks were placed in a 5% CO_2 incubator at 37 °C for cultivation. After 48 h, non-adherent cells were removed and the medium was changed every 3 days until the adherent cells were confluent. The flasks were then placed in a constant temperature shaker at 37 °C and 160 r/min for 16 h to remove microglia and oligodendrocytes. The purity of Ast was identified by staining with anti-glial fibrillary acidic protein (GFAP) antibody, a marker of Ast (purity > 95%).

The OGD/R model was used to simulate in vitro ischemia/reperfusion (I/R)-like conditions. After discarding the complete medium and washing the cells with phosphate buffered saline (PBS), DMEM without glucose was added and the cells were placed in an anaerobic incubator (0.1% O_2, 5% CO_2, and 94% N_2) at 37 °C for 8 h. After the OGD period, glucose was supplemented to normal levels. The cells were then placed in an incubator with normal growth conditions (5% CO_2 and 95% O_2) at 37 °C and incubated for 24 h. During OGD induction, the OGD/R + HSYA group was treated with 25 μmol/L HSYA for 8 h. The HSYA dose is according to our preliminary series research results. In

the Normal group, the same volume of high-sugar complete culture medium was added instead of HSYA.

Assessment of neurological dysfunction

Neurological dysfunction was assessed in rats 24 h after MCAO/R according to Referencing Longa and Bederson's 5-point scale method: 0 points indicated no symptoms of neurological damage; 1 point indicated an inability to fully extend contralateral forepaw; 2 points indicated circling towards the contralateral side; 3 points indicated tilting towards the contralateral side; and 4 points indicated an inability to walk spontaneously, loss of consciousness. In order to evaluate coordination function of rats, the corner turning test was performed. Firstly, rat was left in the test device consisting of two vertical boards at a 30°angle. When entering the corner, the rats will turn left or right. Under normal conditions, rat turned left or right with equal frequency, but the rat suffered from MCAO/R preferentially turned toward the unimpaired. This test was repeated 10–15 times, with an interval of more than 30 s. The number of turns in each direction of the rats was observed and recorded.

2, 3, 5-Triphenyltetrazolium chloride (TTC) staining

After 24 h of reperfusion, rats were anesthetized and decapitated quickly. Brains were then rapidly removed and placed in a −20 °C freezer. The brains were cut along the coronal axis into seven consecutive sections, each 2 mm thick, and immersed in a 1% TTC solution at 37 °C for 15 min. Normal brain tissue stained red, while the infarcted areas stained white. Images of the tissues were captured using a camera, and the area of infarction was measured using Image J 8.0 software.

Hematoxylin-Eosin (HE) staining

After anesthesia, the hearts were slowly perfused with normal saline and 4% paraformaldehyde solution. After decapitation, the brain tissue was stripped, fixed, dehydrated, and embedded in paraffin. The paraffin-embedded brain tissues were cut into 10 μm thick sections and dewaxed by successive washes in xylene, anhydrous ethanol, and gradient alcohol. The sections were stained with HE stain according to the standard procedure. Briefly, the slices were washed in 95% alcohol, anhydrous ethanol, and transparent with xylene dehydration, slightly dried, and then sealed with neutral gum. The slices were observed under a microscope and images were analyzed using ImageJ.

Western blot (WB) analysis

Brain tissues were homogenized using radioimmunoprecipitation analysis (RIPA) Lysis Buffer. Following the addition of phenylmethylsulfonyl fluoride (PMSF) and phosphatase inhibitors, the lysate was cooled on ice for 30 min in preparation of Western blotting. The One-Step Polyacrylamide Gel Electrophoresis (PAGE) Gel Fast Preparation Kit was used to prepare a 6–15% gradient gel for electrophoresis, and the protein was subsequently transferred to a polyvinylidene difluoride (PVDF) membrane. The membrane was first incubated in skim milk at room temperature (RT) for 1 h and then incubated in specific primary antibody in a 4 °C shaker overnight. The membrane was finally incubated in a secondary antibody at RT for 1.5 h.

Immunoblots were developed with an enhanced chemiluminescence system and measured using Quantity Software.

Immunofluorescence (IF) staining

To perform IF staining on brain slices, the brain tissues were embedded in paraffin for sectioning. The sections were then dewaxed using xylene and alcohol, followed by antigenic repair using sodium citrate solution, before IF staining. To perform IF staining on cells, the culture medium was discarded, and the cells were rinsed with PBS. They were then fixed in 4% paraformaldehyde for 30 min and subjected to IF staining. Both the brain sections and cell slides were permeabilized and blocked with PBS containing 0.1% Triton X-100 and 3% bovine serum albumin (BSA) at RT for 1.5 h. They were then incubated overnight with specific primary antibodies at 4 °C. Finally, the samples were incubated with fluorescein-conjugated secondary antibodies at RT for 1.5 h and observed using a fluorescence microscope or confocal microscope.

Enzyme-linked immunosorbent assay (ELISA)

The concentrations of cytokines in the brain tissue extracts and cell culture supernatants were measured using sandwich ELISA kits following the manufacturer's instructions. Determinations were performed in duplicates, and the results were expressed as pg/ml.

Terminal deoxynucleotidyl transferase dUTP Nick end labeling (TUNEL) staining

In accordance with the manufacturer's instructions, apoptosis was assessed using a TUNEL kit. After removing the culture medium and washing with PBS, the cells were fixed in 4% paraformaldehyde for 30 min. Subsequently, they were permeabilized with PBS with 0.3% Triton X-100 for

15 min before being exposed to the TUNEL assay solution at 37 °C for 1 h. The nuclei of TUNEL-positive cells were examined with a fluorescence microscope and quantified with Image-Pro Plus 5.0.

Gene knockdown by ShRNA

Primary Ast were inoculated into 12-well plates at a density of 4×10^5 cells/well, and carrier plasmids carrying shRNA-STAT3 & OE-LCN2 (HANBIO, China) were transfected into Ast using LipofiterTM transfection reagent (HANBIO, China). After 24 h, the transfection medium was replaced with DMEM, and the cells were incubated for an additional 24–48 h. To verify the effectiveness of shRNA, the expression level of STAT3 protein was detected by fluorescence staining and Western Blot.

Statistical analyses

Statistical analyses were performed using GraphPad Prism 8.0 software (USA). All values are expressed as mean ± standard deviation. One-way ANOVA and post hoc least significant difference multiple comparison tests were used to compare more than two groups. $p < 0.05$ was considered statistically significant.

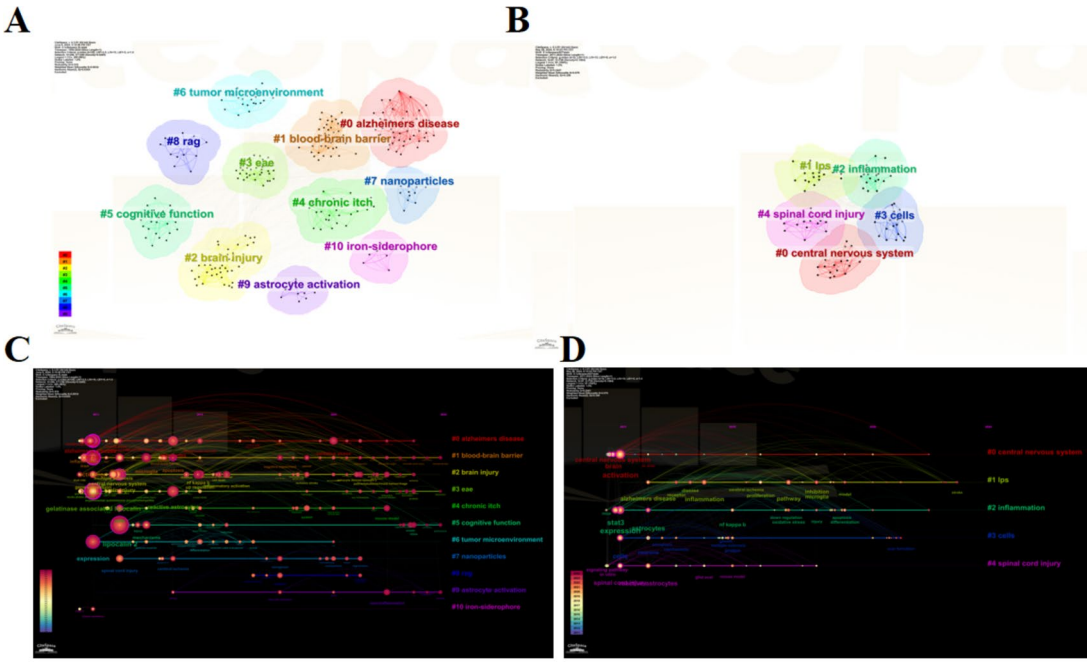

E Top 25 Keywords with the Strongest Citation Bursts

Keywords	Year	Strength	Begin	End	2011 - 2024
acute phase protein	2011	1.81	2011	2015	
choroid plexus	2012	1.94	2012	2015	
in vivo	2012	1.23	2012	2013	
experimental allergic encephalomyelitis	2012	1.14	2012	2014	
cd8(+) t cells	2012	1.14	2012	2014	
receptor	2012	1.13	2012	2013	
amyotrophic lateral sclerosis	2013	1.78	2013	2014	
alzheimers disease	2011	1.1	2013	2014	
gene expression	2011	1.4	2015	2016	
activated microglia	2015	1.14	2015	2016	
closed head injury	2017	1.2	2017	2018	
inflammation	2011	2.73	2018	2019	
cerebral ischemia	2014	1.29	2018	2019	
system	2019	2.62	2019	2020	
up regulation	2015	1.41	2019	2020	
astrocytes	2014	2.37	2020	2021	
oxidative stress	2020	2.26	2020	2024	
reactive astrocytes	2014	1.48	2020	2021	
astrocyte derived lipocalin 2	2021	1.84	2021	2022	
brain injury	2012	1.81	2021	2022	
inflammatory activation	2016	1.71	2021	2024	
nf kappa b	2015	3.3	2022	2024	
neuroinflammation	2022	2.62	2022	2024	
mouse model	2022	2.55	2022	2024	
subarachnoid hemorrhage	2022	2.12	2022	2024	

F Top 25 Keywords with the Strongest Citation Bursts

Keywords	Year	Strength	Begin	End	2011 - 2024
central nervous system	2011	6.48	2011	2015	
in vitro	2011	6.31	2011	2015	
fibrillary acidic protein	2011	5.36	2011	2016	
gene expression	2011	5.34	2011	2013	
oxidative stress	2017	5.12	2021	2022	
nf kappa b	2015	5.03	2015	2018	
proliferation	2016	4.67	2016	2019	
receptor	2013	4.65	2021	2024	
microglia	2018	4.39	2021	2024	
inhibition	2018	4	2022	2024	
alzheimers disease	2012	3.94	2017	2018	
down regulation	2017	3.92	2017	2020	
neural stem cells	2015	3.89	2015	2016	
nitric oxide synthase	2011	3.74	2011	2012	
mechanisms	2013	3.66	2020	2021	
apoptosis	2019	3.64	2019	2020	
astrocyte differentiation	2013	3.57	2013	2014	
disease	2014	3.52	2021	2024	
protein	2015	3.49	2020	2021	
scar formation	2021	3.43	2021	2024	
multiple sclerosis	2015	3.38	2021	2022	
model	2019	3.38	2022	2024	
in vivo	2012	3.27	2012	2018	
nervous system	2013	3.17	2013	2016	
neurons	2012	2.92	2012	2016	

Fig. 2 (**A**) Yearly postings including the terms STAT3 and astrocytes. (**B**) Yearly postings including the terms LCN2 and astrocytes. (**C**) Keyword co-occurrence of STAT3 and astrocytes. (**D**) Keyword co-occurrence of LCN2 and astrocytes. (**E**) Timeline analysis of keyword clustering of STAT3 and astrocytes. (**F**) Timeline analysis of keyword clustering of LCN2 and astrocytes

Results

Analysis of results from papers published between 2011 and 2024

A temporal analysis of papers published between 2011 and 2024 showed a fluctuating upward trend in the number of papers, which may reflect an increasing interest in the Ast-STAT3 and Ast-LCN2 relationships (Fig. 2A & B). Keywords such as "inflammation," "astrocytes," "STAT3," "LCN2," and "neuroprotection" emerged as central nodes in the co-occurrence network, reflecting the core themes of research in this field (Fig. 2C & D). The timeline analysis revealed that certain keywords emerged as prominent nodes at various intervals along the X-axis, with each node encapsulating a year's research output. The size of the node is indicative of the intensity of research interest, and it is notable that the research on STAT3 and LCN2 stands out as a particularly hot topic within the field (Fig. 2E & F). These visualizations and analyses provided guidance with which subsequent in vitro and in *vivo* experiments were designed.

Treatment with HSYA alleviated neuronal damage following ischemic stroke

The neurological scores of rats in each group was evaluated (Fig. 3A). The results showed that HSYA intervention inhibited the increase in MCAO/R-induced neurological scores compared with the Sham group. The Corner Turning Test confirmed this conclusion (Fig. 3B). TTC staining revealed a decline in cerebral infarction volume in MCAO/R model rats treated with HSYA (Fig. 3C). HE staining of the rats hippocampus showed irregular neuronal arrangement, cytoplasmic atrophy, and nuclear depth staining atrophy following MCAO/R, indicating that the neuronal damage was aggravated (Fig. 3D). After HSYA treatment, the neuronal damage was alleviated. Similarly, TUNEL staining showed that neuronal apoptosis was significantly increased in the MCAO/R group compared to those in the Sham group, and treatment with HSYA reduced the degree of neuronal apoptosis induced by MCAO/R (Fig. 3E).

HSYA inhibited the expression of LCN2 and inflammatory factors in Ast after MCAO/R

Western Blot analysis showed that the expression of LCN2 protein was increased in the MCAO/R group, while the expression of LCN2 protein in the MCAO/R + HSYA group was decreased by comparison (Fig. 4A). Double staining with LCN2 and GFAP in brain slices showed that LCN2 was mainly expressed in GFAP-positive Ast (Fig. 4B). Compared with the Sham group, the expression of LCN2 in the Ast was significantly increased following MCAO/R. HSYA treatment partially mitigated this effect, with the expression of LCN2 in the Ast treated with HSYA lower than that in non-treated Ast. These results indicate that LCN2 expression in Ast is induced by MCAO/R and inhibited by HSYA treatment.

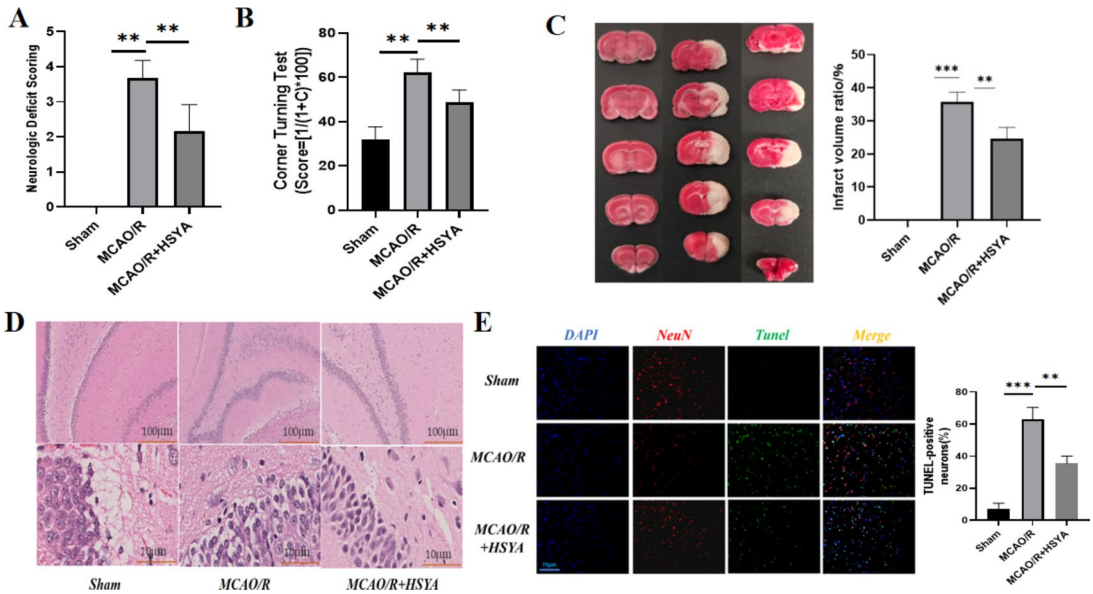

Fig. 3 (**A**) Neurological deficits in rats were evaluated based on the neurological grading scale. (**B**) The Corner Turning Test was conducted 24 h post-reperfusion. (**C**) Cerebral infarction volume in rats was determined through TTC staining, with statistical analysis conducted using ImageJ. (**D**) HE staining was carried out in the hippocampal regions of rats. (**E**) Representative microphotographs and quantitative analysis of TUNEL-positive neurons in the ischemic penumbra 24 h after MCAO/R. Results are expressed as the means ± SD. ** $p < 0.01$, *** $p < 0.001$

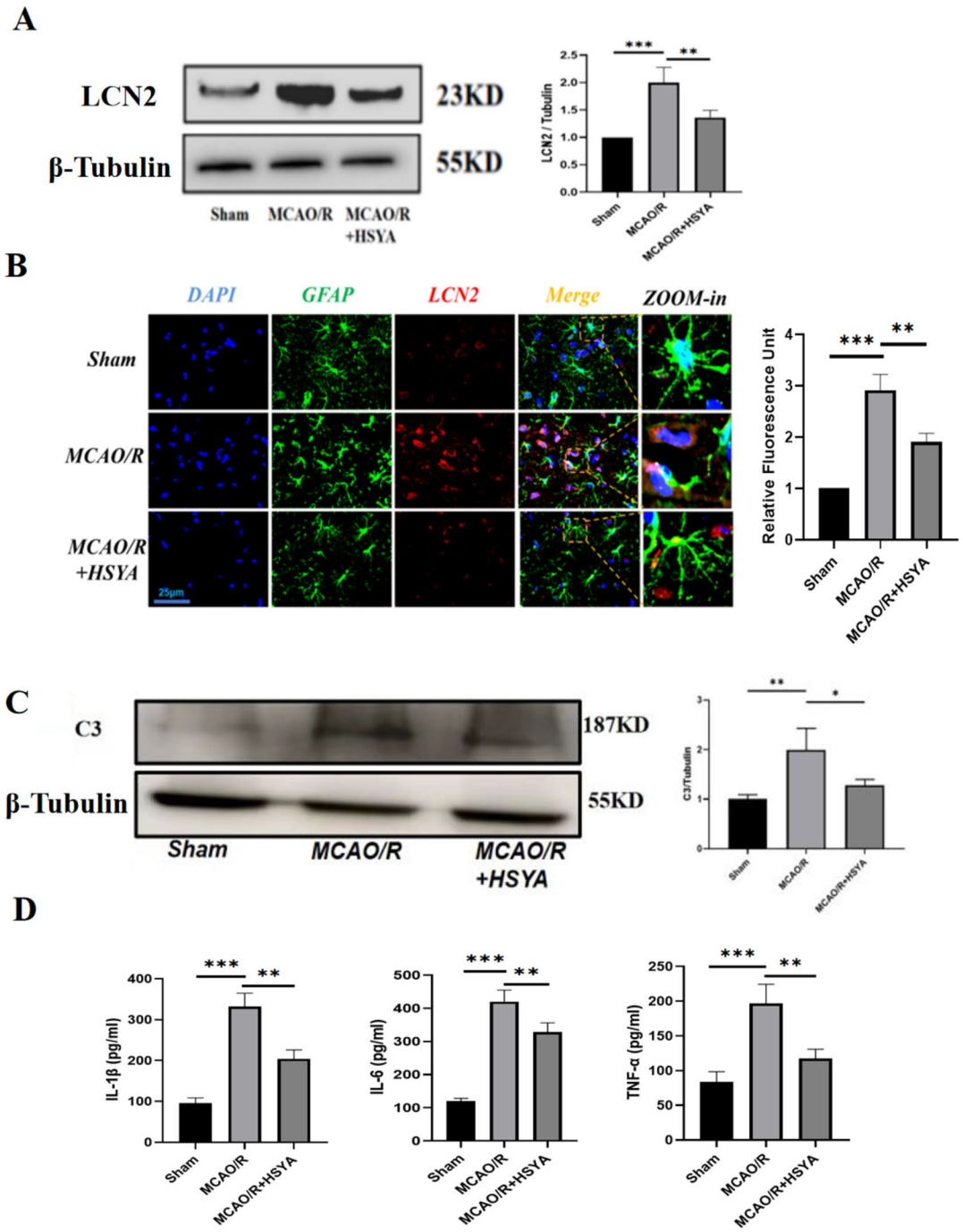

Fig. 4 (**A**) Expression levels of LCN2 protein. (**B**) Representative IF staining of GFAP (green) and LCN2 (red) in Ast after MCAO/R (2 h/24 h) in rats. (**C**) Expression level of C3 protein. (**D**) Expression levels of IL-1β, IL-6, and TNF-α determined by ELISA. Results are expressed as the means ± SD. *$p<0.05$, ** $p<0.01$, *** $p<0.001$

To investigate the effect of HSYA treatment on MCAO/R-induced inflammatory response in brain, Western blotting was used to detect the levels of inflammatory cytokines (Fig. 4C). The results showed that the protein expression of C3 increased following MCAO/R and treatment with HSYA inhibited this increase, suggesting that MCAO/R induces pro-inflammatory changes in Ast that can be mitigated by HSYA. ELISA detection of inflammatory cytokine levels in rat brain homogenate revealed that, compared with Sham group, the serum levels of IL-1β, IL-6, and TNF-α in the MCAO/R group were increased. Notably, the serum levels of these inflammatory factors decreased following HSYA intervention, indicating that HSYA also inhibited the circulating inflammatory response after MCAO/R (Fig. 4D).

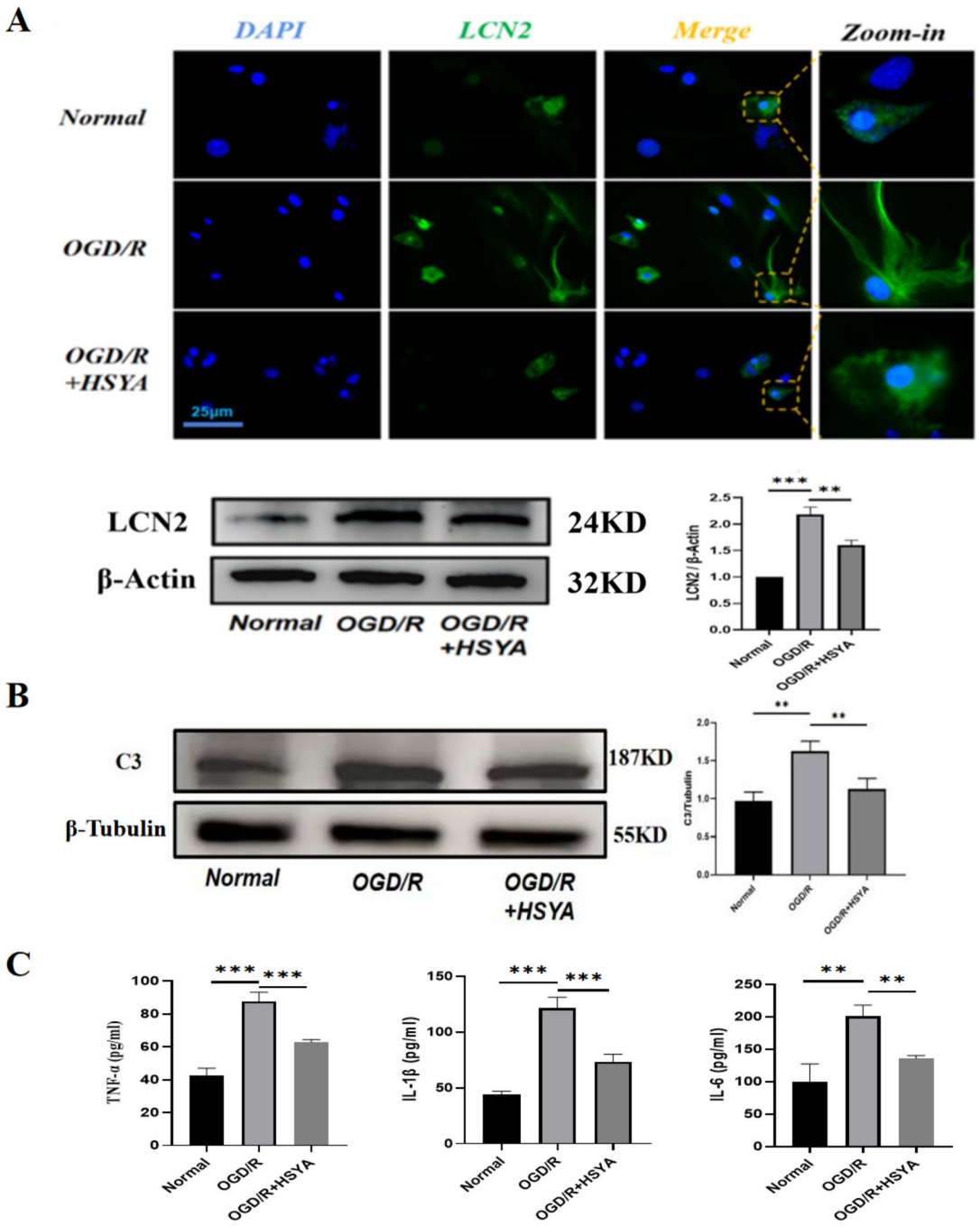

Fig. 5 (**A**) Representative IF images of LCN2 (green) and Western blot analysis of LCN2 protein expression levels after OGD/R (8 h/24 h) in vitro. (**B**) Western blot analysis of C3. (**C**) Expression levels of TNF-α, IL-1β, and IL-6 determined by ELISA. Results are expressed as the means ± SD. *$p < 0.05$, ** $p < 0.01$, *** $p < 0.001$

LCN2 and inflammatory cytokine expression levels were elevated in Ast following OGD/R

To further verify the effect of OGD/R on Ast, cell-based assays were used. The results show that the expression of LCN2 protein in Ast increased after OGD/R, while HYSA treatment inhibited its expression (Fig. 5. A). Moreover, Western blotting and IF analyses showed that while the expression of C3 protein was increased in the OGD/R group, the expression level was decreased in the OGD/R + HSYA group by comparison (Fig. 5B). ELISA confirmed that the levels of the inflammatory cytokines IL-1β, IL-6, and TNF-α were also increased following OGD/R (Fig. 5C), and that HSYA treatment effectively inhibited their expressions. These results suggest that OGD/R induces the expression of

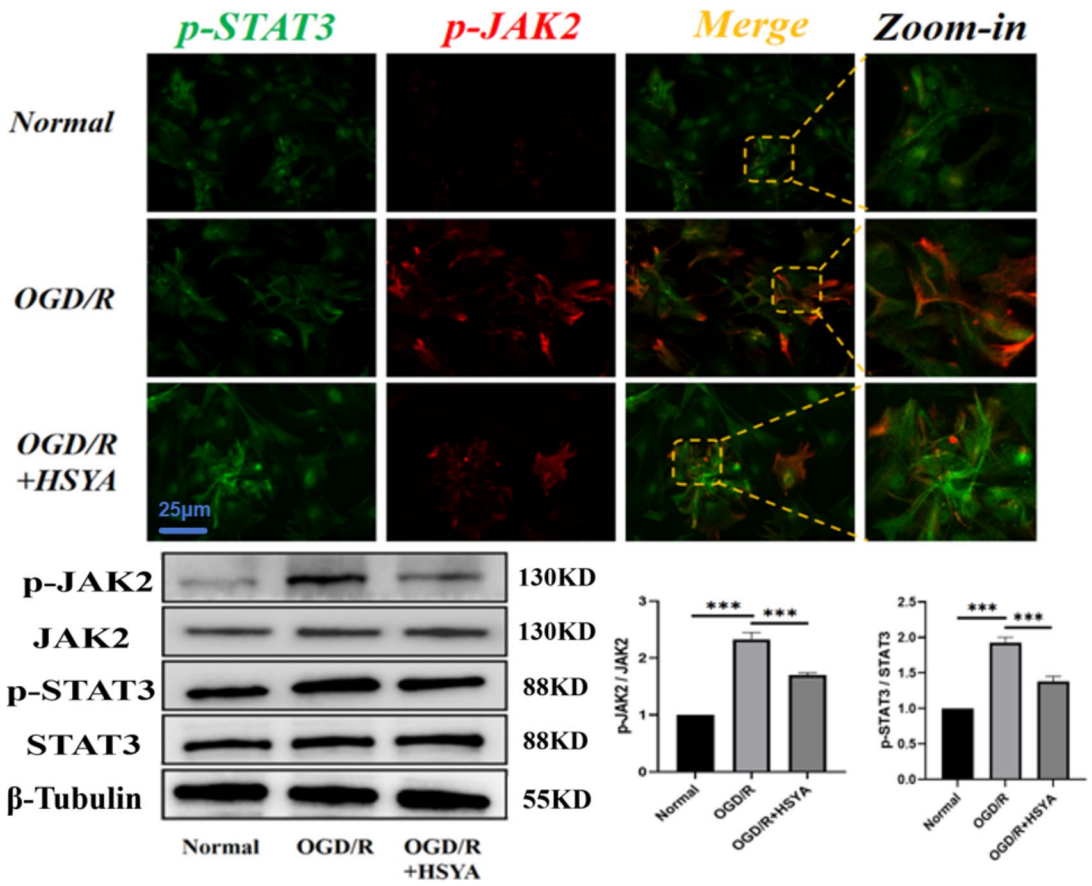

Fig. 6 Representative IF images of p-STAT3 (green) and p-JAK2 (red) and Western blot analysis of p-JAK2, JAK2, p-STAT3, and STAT3 protein *expression* levels after OGD/R in vitro. Results are expressed as the means ± SD. *** $p < 0.001$

LCN2 in Ast, stimulates the increase of the inflammatory molecules such as C3, TNF-α, IL-6, and IL-1β, and triggers the inflammatory response of Ast after OGD/R, all of which can be mitigated by treatment with HSYA.

JAK2/STAT3 was activated by phosphorylation in Ast following OGD/R

JAK2/STAT3 is involved in the signal transduction of various inflammatory responses. To examine whether JAK2/STAT3 is activated in Ast following OGD/R, the expression levels of both total and phosphorylated (p-) JAK2 and STAT3 were measured. As expected, both IF and Western blot analyses showed that the expression of p-JAK2 and p-STAT3 were upregulated, indicating that OGD/R induced the activation of the JAK2/STAT3 in Ast (Fig. 6).

Knockdown of the JAK2 / STAT3 pathway inhibited LCN2 expression

As previously mentioned, LCN2 can induce the activation of JAK2/STAT3. In a recent study, it was observed that alcohol upregulated extrahepatic IL-6, resulting in STAT3 activation in hepatocytes and downstream LCN2 up-regulation (Qiu et al. 2023). To determine whether activation of JAK2/STAT3 affects LCN2 expression following OGD/R and whether there exists a feedback loop between JAK2/STAT3 and LCN2, STAT3 expression was disrupted in Ast using an adenovirus-based short hairpin RNA (shRNA) system (Fig. 7A). Interestingly, the expression of LCN2 protein in STAT3 knockdown (shSTAT3) Ast was significantly decreased following OGD/R (Fig. 7B). These findings indicate that not only does LCN2 induce JAK2/STAT3 activation, but also that STAT3 can in turn regulate the expression of LCN2, demonstrating the existence of a positive feedback loop between LCN2 and JAK2/STAT3.

HSYA-mediated suppression of LCN2 expression in Ast inhibited the activation of the JAK2/STAT3 following OGD/R

The positive feedback loop between LCN2 and the JAK2/STAT3 was activated following ischemic stroke, resulting in the further development of neuroinflammation. By contrast, treatment with HSYA effectively inhibited both the expression of LCN2 protein and the activation of JAK2/STAT3

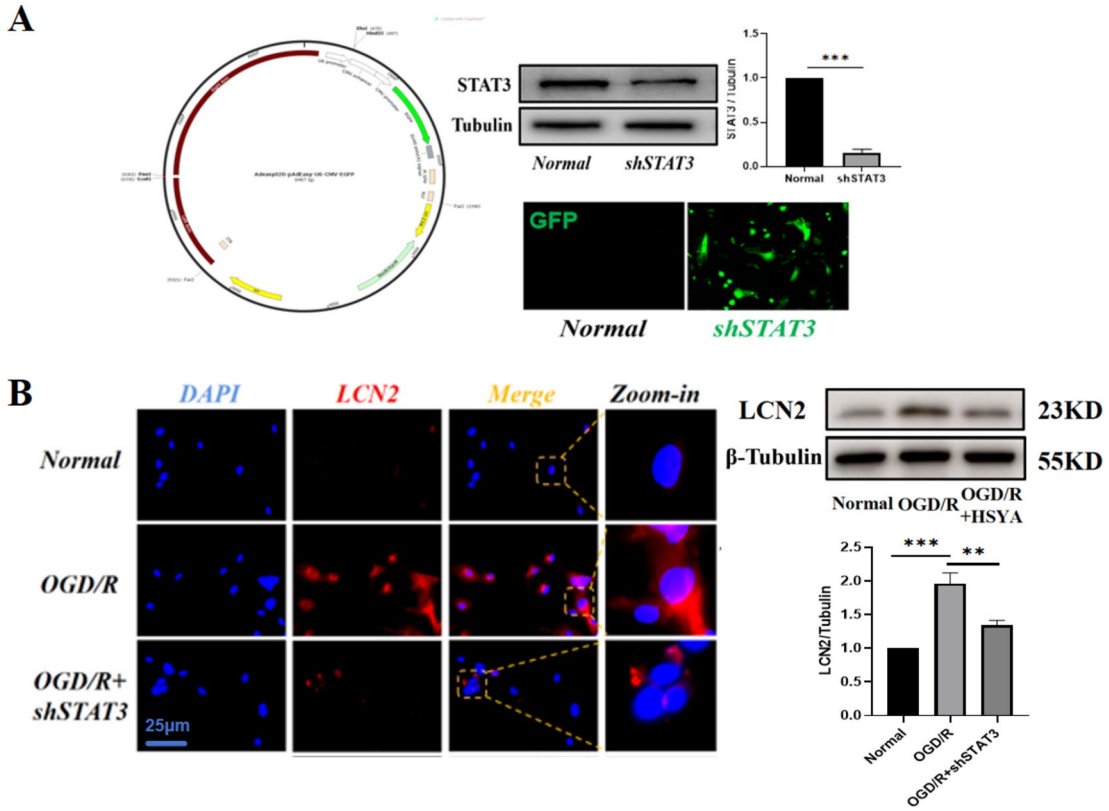

Fig. 7 (**A**) Adenovirus-mediated transfection of shSTAT3 in Ast knocked down STAT3 expression. (**B**) Representative IF images of LCN2 (red) after OGD/R in vitro. Western blot analysis of STAT3 and LCN2 protein expression levels. Results are expressed as the means ± SD. $^{**}p < 0.01$, $^{***}p < 0.001$

following ischemic stroke. These two findings raise an interesting question: Can HSYA treatment block the activation of JAK2/STAT3 following OGD/R by inhibiting the expression of LCN2 in Ast? To answer this question, an adenoviral system was used to overexpress LCN2 in Ast. Western blotting analysis showed that HSYA treatment reduced the inflammatory response in Ast following OGD/R via inhibition of the LCN2/STAT3 loop (Fig. 8).

Discussion

Ischemic stroke has a high rate of disability and mortality and can cause sequelae and complications that seriously affect patient's quality of life which can lead to social and economic burden. While thrombolysis is an effective strategy if operated within a critical time window following stroke, the resulting reperfusion injury caused by thrombolysis can trigger inflammatory and oxidative stress reactions, leading to further neurological damage (Orellana-Urzúa et al. 2020; Chen et al. 2020). The neuroinflammation caused by reperfusion develops over hours or even months, often transforming from acute inflammatory response into sustained chronic inflammation. The long-term presence of neuroinflammation represents a crucial underlying risk factor that needs adequate treatment attention (Shi et al. 2019).

LCN2 plays a key role in I/R injury and is closely related to the expression of iNOS. iNOS expressed in Ast can generate nitric oxide (NO), which directly reacts with reactive oxygen species (ROS) to form cytotoxic peroxynitrite anions (ONNO-) that damage mitochondrial enzymes and genetic material (Wierońska et al. 2021). Evidence suggests that neither LCN2 mRNA nor LCN2 protein are present in the brain under non-ischemic conditions. Instead, their expression is upregulated following ischemic-hypoxic events and is involved in the neuroinflammatory response. Compared to MCAO/R model mice, LCN2-silenced mice showed a significant decrease in the expression of neuroinflammatory cytokines following MCAO/R (Zhao et al. 2019). Similarly, knockout or knockdown of LCN2 can inhibit or reverse the neuroinflammatory response in mice following traumatic brain injury, hemorrhagic stroke, and experimental autoimmune encephalomyelitis (Jung et al. 2023; Liu et al. 2022b; Gasterich et al. 2022). These findings suggest that LCN2 is a key mediator of neuroinflammation in response to various diseases of the central nervous system (CNS).

Previous studies have indicated that LCN2 is primarily produced by Ast following ischemic stroke (Jin et al. 2014). Our

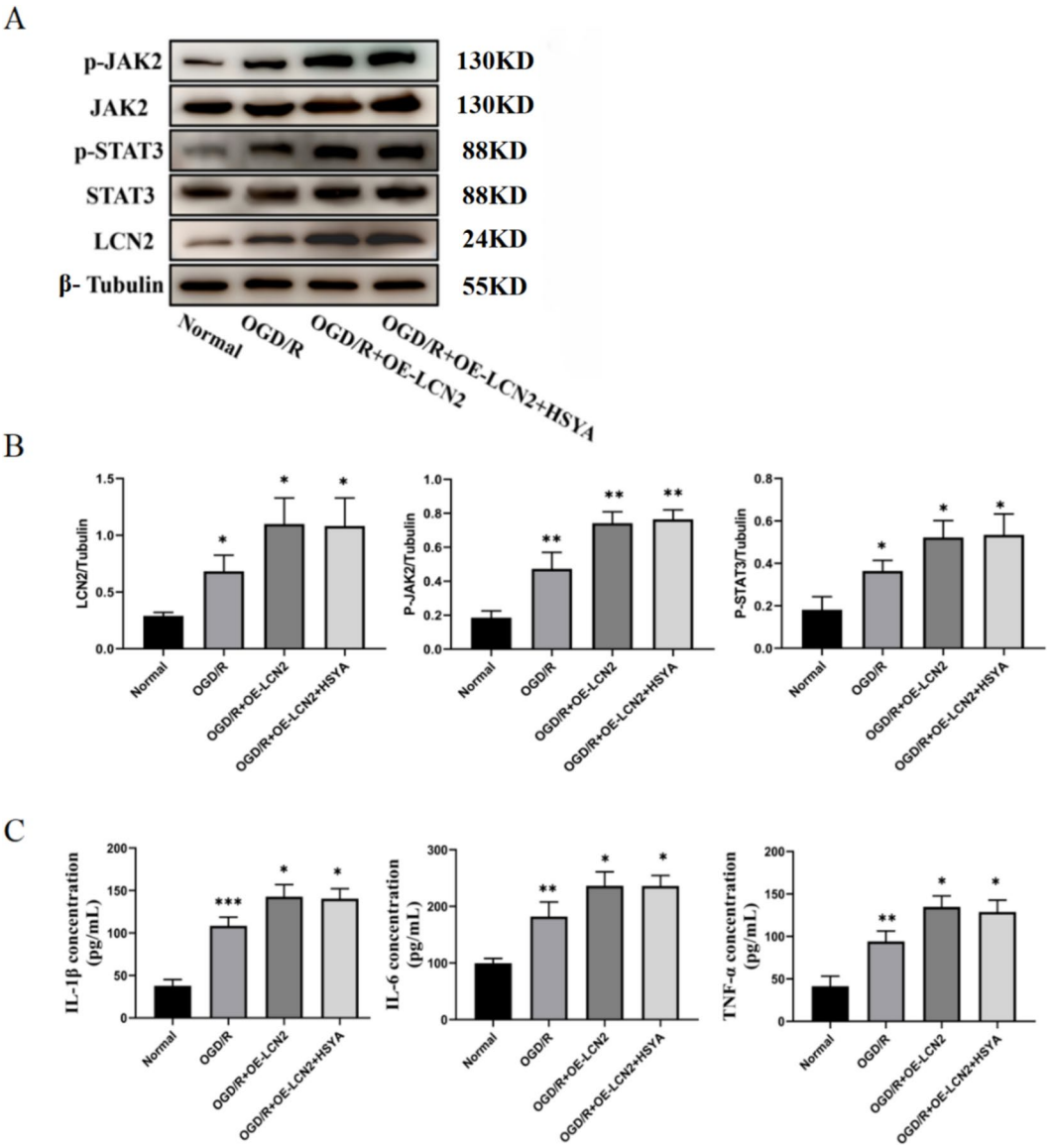

Fig. 8 (**A**) The expression levels of p-JAK2, JAK2, p-STAT3, STAT3, and LCN2 protein determined by Western blot. (**B**) Western blot analysis of p-JAK2, p-STAT3and LCN2. (**C**) Levels of TNF-α, IL-1β, and IL-6 release determined by ELISA. All results are from 3 samples and expressed as the mean ± SD. *$p < 0.05$, **$p < 0.01$, ***$p < 0.001$

findings strongly suggest that LCN2 expression is upregulated in both the in vivo MCAO/R rat model and the in vitro Ast OGD/R model, which in turn leads to the development of an inflammatory phenotype in Ast, involving the secretion of several inflammatory cytokines and exacerbating inflammatory damage in the CNS (Deng et al. 2019). However, the upstream molecules involved in triggering the upregulation of LCN2 in Ast have not been thoroughly explored, especially under MCAO/R and OGD/R conditions. Previous studies have shown that JAK2/STAT3 is activated in Ast after ischemic stroke alongside an increase in the expression of pro-inflammatory LCN2 (Wang et al. 2020). However, the connection between STAT3 and LCN2 has not been well described.

Interestingly, some studies on CNS disease provide evidence for possible crosstalk between the LCN2 and JAK2/STAT3 (Han et al. 2024). Following spinal cord injury, Ast and microglia were found to be activated and played a role in the subsequent pathological process (Bretheau et al. 2022). JAK2/STAT3 phosphorylation is inhibited by LCN2 knockout, and the expression of LCN2 can be downregulated by inhibition of JAK2/STAT3. The inhibition of either LCN2 or JAK2/STAT3 in this process inhibited Ast and microglia activation and reduced neurotoxicity (Wang et al. 2021; Zhang et al. 2019). Based on this information, it is tempting to speculate that there may be crosstalk between LCN2 and JAK2/STAT3 in Ast. As such, it is reasonable to speculate

that the interaction between LCN2 and JAK2/STAT3 could synergistically activate pro-inflammatory responses, thereby exacerbating Ast-derived neuroinflammatory injury.

Through both in vivo MCAO/R rat and in vitro primary astrocyte OGD/R models, we demonstrated a positive correlation between LCN2 and JAK2/STAT3. Crosstalk between the LCN2 and JAK2/STAT3 was found to influence astrocytic functional activation and plays a role in subsequent inflammatory responses, while treatment with HSYA inhibited LCN2 expression and JAK2/STAT3 activation following MCAO/R and OGD/R. We also used an adenoviral system to overexpress LCN2 or silence STAT3 in Ast in order to better understand the interaction between LCN2 and STAT3. These experiments demonstrated that upregulation of LCN2 activated the phosphorylation of STAT3 while silencing of STAT3 inhibited the secretion of inflammatory cytokines by Ast. These findings suggest a synergistic relationship between LCN2 and STAT3 that affects the Ast inflammatory response following ischemic stroke.

HSYA treatment has been shown to downregulate the expression of LCN2 and inhibit the activation of JAK2/STAT3 by disrupting the LCN2-STAT3 crosstalk following ischemic stroke. This ultimately mitigates Ast-mediated neuroinflammation induced by I/R injury. Therefore, targeting Ast to block the synergistic relationship between LCN2 and STAT3 may serve as a potential therapy for reducing neuroinflammation and protecting neurological function in ischemic stroke. To this end, HSYA represents a promising potential drug to treat neuroinflammatory injury following ischemic stroke. We speculate HSYA may directly bind to LCN2 or JAK2/STAT3, which is also we need to further study in the future.

Conclusions

Following ischemic stroke, there is an interaction between the LCN2 and JAK2/STAT3 in Ast that results in an increase in the expression of inflammatory factors and exacerbates neuroinflammatory injury. However, HSYA can inhibit this interaction, thereby mitigating neuroinflammation post-ischemic stroke.

Supplementary Information The online version contains supplementary material available at https://doi.org/10.1007/s11011-025-01581-2.

Acknowledgements We thank LetPub (www.letpub.com.cn) for its linguistic assistance during the preparation of this manuscript.

Author contributions LJ Song, LJ Yin, YG Wu, KX Liu, YZ Duan and JL Hua conducted experiments. LJ Song drafted the manuscript. JJ Yin, YG Wu, KX Liu，MW Rong and D Ma analyzed data. C Zhang, CG Ma and BG Xiao designed the experiments and revised and finalized the manuscript. All authors have read and agreed to the published version of the manuscript.

Funding This work was supported by China Postdoctoral Science Foundation (2020M680912); National Natural Science Foundation of China (82004028); Zhang Zhongjing inheritance and Innovation Project of State Administration of Traditional Chinese Medicine (GZY-KJS-2022-048-1); Science and Technology Cooperation and Exchange Special Project of Shanxi Province in 2023 (202304041101004);Shanxi Science and Technology Innovation Young team Project (202204051001028); Science and Technology Innovation Team Project of Shanxi University of Chinese Medicine (2022TD2010); Cardiovascular Special Fund Project of The National Regional Medical Center of Traditional Chinese Medicine and Affiliated Hospital of Shanxi University of Chinese Medicine (XGZX202115); Shanxi University of Chinese Medicine Science and Technology Innovation Capability Cultivation Plan National Natural Science Foundation Cultivation Special Project (2024PY-NS-012); and Discipline construction funds of Shanxi University of Chinese Medicine (2024XKJS-02).

Data availability No datasets were generated or analysed during the current study.

Declarations

Competing interests The authors declare no competing interests.

References

Adly Sadik N, Ahmed Rashed L, Abd-El Mawla A, M., et al (2021) Circulating miR-155 and JAK2/STAT3 axis in acute ischemic stroke patients and its relation to post-ischemic inflammation and associated ischemic stroke risk factors. Int J Gen Med 14:1469–1484. https://doi.org/10.2147/IJGM.S295939

Ajoolabady A, Wang S, Kroemer G, Penninger JM, Uversky VN, Pratico D, Henninger N, Reiter RJ, Bruno A, Joshipura K, Aslkhodapasandhokmabad H, Klionsky DJ, Ren J et al (2021) Targeting autophagy in ischemic stroke: From molecular mechanisms to clinical therapeutics. Pharmacol Ther 225:107848. https://doi.org/10.1016/j.pharmthera.2021.107848

Bretheau F, Castellanos-Molina A, Mailhot B, Boisvert A,Vallières N, Lessard MGMLX, Boilard É, Quan N, Lacroix S et al (2022) The alarmin interleukin-1α triggers secondary degeneration through reactive astrocytes and endothelium after spinal cord injury. Nat Commun 13:5786. https://doi.org/10.1038/s41467-022-33463-x

Chen H, He Y, Chen S, Qi S, Shen J et al (2020) Therapeutic targets of oxidative/nitrosative stress and neuroinflammation in ischemic stroke: applications for natural product efficacy with omics and systemic biology. Pharmacol Res 158:104877. https://doi.org/10.1016/j.phrs.2020.104877

Deng Y, Chen D, Gao F, Lv H, Zhang G, Sun X, Liu L, Mo D, Ma N, Song L, Huo X, Yan T, Zhang J, Miao Z et al (2019) Exosomes derived from microRNA-138-5p-overexpressing bone marrow-derived mesenchymal stem cells confer neuroprotection to astrocytes following ischemic stroke via Inhibition of LCN2. J Biol Eng 13:71. https://doi.org/10.1186/s13036-019-0193-0

Gasterich N, Bohn A, Sesterhenn A, Nebelo F, Fein L, Kaddatz H, Nyamoya S, Kant S, Kipp M, Weiskirchen R, Zendedel A, Beyer C, Clarner T et al (2022) Lipocalin 2 attenuates oligodendrocyte loss and immune cell infiltration in mouse models for multiple sclerosis. Glia 70:2188–2206. https://doi.org/10.1002/glia.24245

Ha GH, Kim EJ, Park JS, Kim JE, Nam H, Yeon JY, Lee SH, Lee K, Kim CK, Joo KM et al (2022) JAK2/STAT3 pathway mediates neuroprotective and pro-angiogenic treatment effects of adult human neural stem cells in middle cerebral artery occlusion stroke animal models. Aging 14:8944–8969. https://doi.org/10.18632/aging.204410

Han B, An Z, Gong T, Pu Y, Liu K et al (2024) LCN2 promotes proliferation and glycolysis by activating the JAK2/STAT3 signaling pathway in hepatocellular carcinoma. Appl Biochem Biotechnol 196: 717–728. https://doi.org/10.1007/s12010-023-04520-y

Jin M, Kim JH, Jang E, Lee YM, Soo Han H, Woo DK, Park DH, Kook H, Suk K et al (2014) Lipocalin-2 deficiency attenuates neuroinflammation and brain injury after transient middle cerebral artery occlusion in mice. J Cereb Blood Flow Metab 34:1306–1314. https://doi.org/10.1038/jcbfm.2014.83

Jung BK, Park Y, Yoon B, Bae JS, Han SW, Heo JE, Kim DE, Ryu KY et al (2023) Reduced secretion of LCN2 (lipocalin 2) from reactive astrocytes through autophagic and proteasomal regulation alleviates inflammatory stress and neuronal damage. Autophagy 19:2296–2317. https://doi.org/10.1080/15548627.2023.2180202

Kido R, Hiroshima Y, Kido JI, Ikuta T, Sakamoto E, Inagaki Y, Naruishi K, Yumoto H et al (2020) Advanced glycation end-products increase Lipocalin 2 expression in human oral epithelial cells. J Periodontal Res 55:539–550. https://doi.org/10.1080/15548627.2023.2180202

Liu H, Li J, Jiang L, He J, Zhang H, Wang K et al (2022a) Dexmedetomidine pretreatment alleviates cerebral ischemia/reperfusion injury by inhibiting neuroinflammation through the JAK2/STAT3 pathway. Braz J Med Biol Res 55:e12145. https://doi.org/10.1590/1414-431X2022e12145

Liu R, Wang J, Chen Y, Collier JM, Capuk O, Jin S, Sun M, Mondal SK, Whiteside TL, Stolz DB, Yang Y, Begum G et al (2022b) NOX activation in reactive astrocytes regulates astrocytic LCN2 expression and neurodegeneration. Cell Death Dis 13:371. https://doi.org/10.1038/s41419-022-04831-8

Lucas SM, Rothwell NJ, Gibson RM et al (2006) The role of inflammation in CNS injury and disease. Bri J Pharmacol 147:S232–240. https://doi.org/10.1038/sj.bjp.0706400

Luo C, Zhou S, Yin S, Jian L, Luo P, Dong J, Liu E et al (2022) Lipocalin-2 and cerebral stroke. Front Mol Neurosci 15:850849. https://doi.org/10.3389/fnmol.2022.850849

Orellana-Urzúa S, Rojas I, Líbano L, Rodrigo R et al (2020) Pathophysiology of ischemic stroke: role of oxidative stress. Curr Pharm Des 26:4246–4260. https://doi.org/10.2174/1381612826666200708133912

Paul S, Candelario-Jalil E (2021) Emerging neuroprotective strategies for the treatment of ischemic stroke: an overview of clinical and preclinical studies. Exp Neurol 335:113518. https://doi.org/10.1016/j.expneurol.2020.113518

Qiu X, Zhou J, Xu H, Li Y, Ma S, Qiao H, Zeng K, Wang Q, Ouyang J, Liu Y, Ding J, Liu Y, Zhang J, Shi M, Liao Y, Liao W, Lin L et al (2023) Alcohol reshapes a liver premetastatic niche for cancer by extra- and intrahepatic crosstalk-mediated immune evasion. Mol Ther 31:2662–2680. https://doi.org/10.1016/j.ymthe.2023.07.012

Ranjbar Taklimie F, Gasterich N, Scheld M, Weiskirchen R, Beyer C, Clarner T, Zendedel A (2019) Hypoxia induces Astrocyte-Derived Lipocalin-2 in ischemic stroke. Int J Mol Sci 20(6):1271. https://doi.org/10.3390/ijms20061271

Shi K, Tian DC, Li ZG, Ducruet AF, Lawton MT, Shi FD (2019) Global brain inflammation in stroke. Lancet Neurol 18(11):1058–1066. https://doi.org/10.1016/S1474-4422(19)30078-X

Suk K (2016) Lipocalin-2 as a therapeutic target for brain injury: an astrocentric perspective. Prog Neurobiol 144:158–172. https://doi.org/10.1016/j.pneurobio.2016.08.001

Sun Y, Xu DP, Qin Z et al (2018) Protective cerebrovascular effects of hydroxysafflor yellow A (HSYA) on ischemic stroke. Eur J Pharmacol 818:604–609. https://doi.org/10.1016/j.ejphar.2017.11.033

Wang G, Weng YC, Chiang IC, Huang YT, Liao YC, Chen YC, Kao CY, Liu YL, Lee TH, Chou WH (2020) Neutralization of Lipocalin-2 diminishes Stroke-Reperfusion injury. Int J Mol Sci 21(17):6253. https://doi.org/10.3390/ijms21176253

Wang X, Li X, Zuo X, Liang Z, Ding T, Li K, Ma Y, Li P, Zhu Z, Ju C, Zhang Z, Song Z, Quan H, Zhang J, Hu X, Wang Z (2021) Photobiomodulation inhibits the activation of neurotoxic microglia and astrocytes by inhibiting Lcn2/JAK2-STAT3 crosstalk after spinal cord injury in male rats. J Neuroinflammation 18(1):256. https://doi.org/10.1186/s12974-021-02312-x

Wei R, Song L, Miao Z, Liu K, Han G, Zhang H, Ma D, Huang J, Tian H, Xiao B, Ma C (2022) Hydroxysafflor yellow A exerts neuroprotective effects via HIF-1α/BNIP3 pathway to activate neuronal autophagy after OGD/R. Cells 11(23):3726. https://doi.org/10.3390/cells11233726

Wierońska JM, Cieślik P, Kalinowski L (2021) Nitric Oxide-Dependent pathways as critical factors in the consequences and recovery after brain ischemic hypoxia. Biomolecules 11(8):1097. https://doi.org/10.3390/biom11081097

Xu S, Lu J, Shao A, Zhang JH, Zhang J (2020) Glial cells: role of the immune response in ischemic stroke. Front Immunol 11:294. https://doi.org/10.3389/fimmu.2020.00294

Zhang Y, Liu J, Yao M, Song W, Zheng Y, Xu L, Sun M, Yang B, Bensoussan A, Chang D, Li H (2019) Sailuotong capsule prevents the cerebral Ischaemia-Induced neuroinflammation and impairment of recognition memory through Inhibition of LCN2 expression. Oxid Med Cell Longev 2019(8416105). https://doi.org/10.1155/2019/8416105

Zhang J, Zhou R, Cao G, Zhang Y, Xu H, Yang H (2022) Guhong injection prevents ischemic Stroke-Induced Neuro-Inflammation and neuron loss through regulation of C5ar1. Front Pharmacol 13:818245. https://doi.org/10.3389/fphar.2022.818245

Zhang W, Xu M, Chen F, Su Y, Yu M, Xing L, Chang Y, Yan T (2023) Targeting the JAK2-STAT3 pathway to inhibit cGAS-STING activation improves neuronal senescence after ischemic stroke. Exp Neurol 368:114474. https://doi.org/10.1016/j.expneurol.2023.114474

Zhao N, Xu X, Jiang Y, Gao J, Wang F, Xu X, Wen Z, Xie Y, Li J, Li R, Lv Q, Liu Q, Dai Q, Liu X, Xu G (2019) Lipocalin-2 May produce damaging effect after cerebral ischemia by inducing astrocytes classical activation. J Neuroinflammation 16(1):168. https://doi.org/10.1186/s12974-019-1556-7

Zhao RY, Wei PJ, Sun X, Zhang DH, He QY, Liu J, Chang JL, Yang Y, Guo ZN (2023) Role of Lipocalin 2 in stroke. Neurobiol Dis 179:106044. https://doi.org/10.1016/j.nbd.2023.106044

Zhong Y, Yin B, Ye Y, Dekhel OYAT, Xiong X, Jian Z, Gu L (2021) The bidirectional role of the JAK2/STAT3 signaling pathway and related mechanisms in cerebral ischemia-reperfusion injury. Exp Neurol 341:113690. https://doi.org/10.1016/j.expneurol.2021.113690

Zhong Y, Gu L, Ye Y, Zhu H, Pu B, Wang J, Li Y, Qiu S, Xiong X, Jian Z (2022) JAK2/STAT3 axis intermediates microglia/macrophage polarization during cerebral ischemia/reperfusion injury. Neuroscience 496:119–128. https://doi.org/10.1016/j.neuroscience.2022.05.016